Optica Applicata, Vol. XIX, No. 1, 1989

Influence of self- and cross-line saturation and multi-transverse mode operation on averaged power characteristics of a CW-GDL active cavity*

MAREK P. BRUNNÉ

Institute of Fluid-Flow Machines, Polish Academy of Sciences, ul. Gen. J. Fiszera 14, 80–952 Gdańsk, Poland.

The analysis of the multi-line active CW-GDL cavity, based upon the system of rate equations, has been performed in order to estimate the influence of the line self- and cross-saturation, and multi-transverse mode operation on efficiency and output power of CW-GDL. The purpose of the paper was to provide a set of simple analytical formulae relating the laser output power and efficiency to dimensionless parameters describing the state of the optical excitation of mixture, the line saturation effects and transverse-mode diffraction losses. The obtained approximative relations are illustrated by a numerical calculations made for a conventional CW-GDL driven by the products of benzene combustion in compressed air.

1. Introduction

The problem of the description of the process of power extraction from a multi-line cw gasdynamic laser cavity by rate equation has been partially considered in [1]. In paper [1], line self- and cross-saturation effects were neglected and it has been tacitly assumed that all longitudinal modes considered pertain to the same transverse mode. Both these assumptions are vulnerable from the physical viewpoint. In conditions occurring in CW-GDL cavities, the gain(s) and line intensity for all self-sustaining lines attain high values. This suggests that line saturation effects and transverse mode operation should be expected to take place in cavities of the above mentioned devices.

The purpose of the present paper is twofold. It means that the multi-line cavity will be described in two cases: i) when the line saturation effects occur but the cavity operates at a single transverse mode regime; ii) when a certain number of transverse modes are sustained within the resonator, but the line self- and cross-saturation effects are neglected. In both cases, a set of simple analytical formulae for laser overall output power, efficiency, individual line outputs and efficiencies (load coefficients) and, finally, the individual transverse mode output(s) and load coef-

* Main part of this work was performed in the frame of the contract of CNR in the Center of Fluids Dynamics Studies at Polytechnic of Turin, Italy.

ficient(s) (efficiencies) are recovered. The solution of this apparently complex task is obtained from the simplest of the existing mathematical models of active laser cavities, described in terms of Rigrod's [1], [2] rate equation. The analysis is oriented towards application to CO_2 or N_2O CW-GDL system. The simplifying assumptions are chosen treating the above mentioned lasers as a practical analogue of the molecular system under description. Some of the assumptions have a general character [1] and will be listed in the next Section of the paper; the others concern only the problem of line saturation or multi-transverse mode cavity operation and are to be specified separately in the respective Sections.

2. Basic assumptions

The cavity **G** under consideration is schematically shown in Fig. 1. It is composed of two flat parallel mirrors $\mathbf{Z}^+$ and $\mathbf{Z}^-$ whose dispersion properties (light absorption capacity) are described by the known reflectivity coefficients $R^+ \leqslant 1$ and $R^- \leqslant 1$. The values $R^{+,-}$ are considered to be identical for all longitudinal (and transverse) modes under consideration. The mirror length, the distance between mirrors, and the height of laser channel are equal to L_x, L_y and L_z, respectively. The symbols v and c denote the medium and light velocity, respectively.

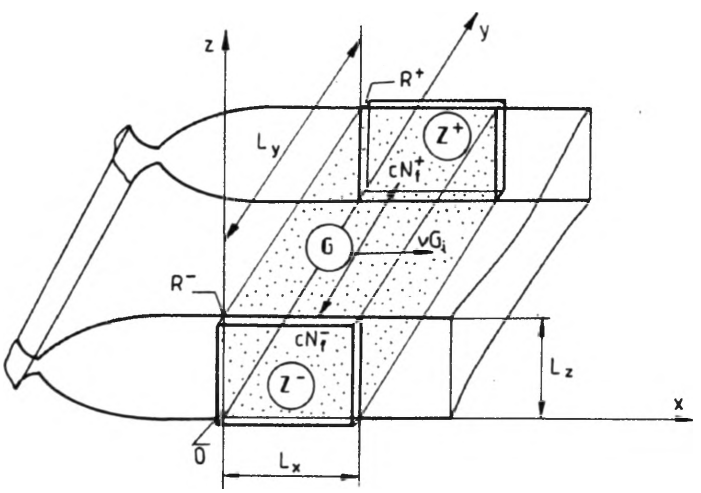

Fig. 1. Geometry of the cavity

It is assumed that macroscopic parameters of the optically activated gas mixture, such as its velocity (v_0), static pressure (p_0), translational temperature (T_0) and partial pressures of the mixture components (x_i) are known and can be treated as constant within the whole region **G** of the optical resonator.

The lasing medium under consideration is by assumption formed by the molecules excited to the upper (m) and lower (n) vibrational levels. The population of each level is treated as being split into rotational sublevels J_i (for the m-level) and J'_i (for the n-level), according to the Maxwell-Boltzman equilibrium distributions

$f_m(T_0, J_i)$ and $f_n(T_0, J_i')$ defined for the rotational temperature equal to the known and constant translational temperature T_0 of the gas mixture. The last assumption of the equilibrium between rotational and translational motion of the molecules in CW-GDL cavities is common for all theoretical calculations concerning CO_2 lasers [3]. The schematic diagram of the lasing medium energy levels is shown in Fig. 2,

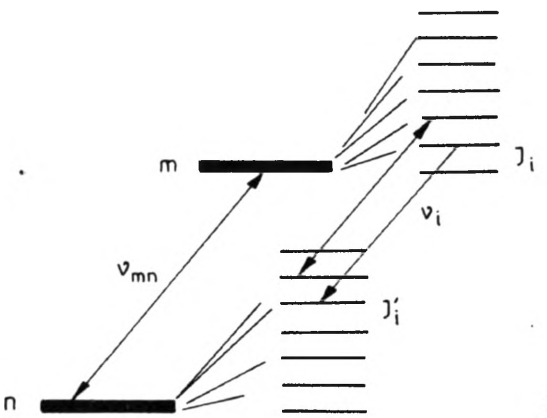

Fig. 2. Schematic diagram of the energy levels

where ν_i ($i = 0, 1, \ldots$) are the central frequencies of the output beam composite lines $(m, J_i) \leftrightarrow (n, J_i')$. The upper and lower groups of the laser levels are characterized by two distinct vibrational temperatures T_m and $T_n < T_m$ or, equivalently, by the population densities $N_m(T_m)$ and $N_n(T_n)$ whose values at the cavity entrance (T_{m0}, T_{n0}, N_{m0}, N_{n0}) are known and constant. Consequently, the values of gain(s) G_{i0} at the cavity inlet cross-section ($x = 0$) can be regarded as known for all interrelated states $(m, J_i) \leftrightarrow (n, J_i')$. It is finally assumed that the changes in gain (G_i) values within the cavity region caused by stimulated emission and absorption processes are mainly balanced by the process of the flow-forced transverse convection of all excited states. The last assumption means that pumping and relaxation processes within the cavity region are neglected. As the gas mixtures used commonly in gasdynamic lasers are supplied with the additives ensuring the effective pumping of the upper laser level and efficient relaxation of the lower laser level, the last assumption is a rather rough simplification. To obtain an upper limit of the CW-GDL output power parameters an alternative case of the ideal pumping of the m-level and ideal depopulation of the n-level is also considered.

3. Influence of the line saturation effects on the multiline cavity operation

3.1. Rate conditions and boundary conditions

Under general assumptions listed in the preceding Section, the CW-GDL cavity (Fig. 1) can be described by a set of non-linear rate equations representing the light

intensity and the (m, J_i) and (n, J_i') level population(s) conservation laws. The above mentioned equations have the following forms [1], [4], [5]:

$$v_0 \frac{\partial N_m(J_i)}{\partial x} = [\bar{B}_{nm}(J_i, J_i') N_n(J_i') - \bar{B}_{mn}(J_i, J_i') N_m(J_i)] (N_{fi}^+ + N_{fi}^-) + \Gamma_{mi}, \tag{1}$$

$$v_0 \frac{\partial N_n(J_i')}{\partial x} = [\bar{B}_{mn}(J_i, J_i') N_m(J_i) - \bar{B}_{nm}(J_i, J_i') N_n(J_i')] (N_{fi}^+ + N_{fi}^-) + \Gamma_{ni}, \tag{2}$$

$$c \frac{\partial N_{fi}^+}{\partial y} = [\bar{B}_{mn}(J_i, J_i') N_m(J_i) - \bar{B}_{nm}(J_i, J_i') N_n(J_i')] N_{fi}^+ - \bar{\beta}_i (N_{fi}^+)^2 - \sum_{j \neq i} \bar{\theta}_{ij} N_{fi}^+ N_{fj}^+, \tag{3}$$

$$c \frac{\partial N_{fi}^-}{\partial y} = [\bar{B}_{nm}(J_i, J_i') N_n(J_i') - \bar{B}_{mn}(J_i, J_i') N_n(J_i)] N_{fi}^- - \bar{\beta}_i (N_{fi}^-)^2 - \sum_{j} \bar{\theta}_{ij} N_{fi}^- N_{fj}^-. \tag{4}$$

Introducing gain G_i assigned to the beam of the central frequency v_i corresponding to $(m, J_i) \leftrightarrow (n, J_i')$ radiative transfer

$$G_i = \left(\frac{1}{c}\right) [\bar{B}_{mn}(J_i, J_i') N_m(J_i) - \bar{B}_{nm}(J_i, J_i') N_n(J_i')], \tag{5}$$

and taking advantage of the assumption that the rotational energy distribution function(s) remains Maxwellian, i.e., putting

$$N_m(J_i) = N_m f_m(T_0, J_i), \quad N_n(J_i') = N_n f_n(T_0, J_i'),$$

the Eqs. (1)–(4) can be rewritten in the following forms [1], [5]:

$$v_0 \frac{\partial G_i}{\partial x} = -[\bar{B}_{mn}(J_i, J_i') f_m(T_0, J_i) + \bar{B}_{nm}(J_i, J_i') f_n(T_0, J_i')] \sum_i G_i (N_{fi}^+ + N_{fi}^-), \tag{6}$$

$$\frac{\partial N_{fi}^+}{\partial y} = G_i N_{fi}^+ - (\bar{\beta}_i / c)(N_{fi}^+)^2 - \sum_{j \neq i} (\bar{\theta}_{ij}/c) N_{fi}^+ N_{fj}^+, \tag{7}$$

$$\frac{\partial N_{fi}^-}{\partial y} = -G_i N_{fi}^- + (\bar{\beta}_i / c)(N_{fi}^-)^2 + \sum_{j \neq i} (\bar{\theta}_{ij}/c) N_{fi}^- N_{fj}^-. \tag{8}$$

While recovering Equation (6) from Eqs. (1), (2) and (5), it has been assumed that the flow forced convection can be regarded within the cavity as a preponderant source of the vibrational energy and therefore

$$\sum_i \Gamma_{mi} \simeq 0, \quad \sum_i \Gamma_{ni} \simeq 0.$$

The starting system of Equations (6) (8) has to be solved together with the boundary conditions specifying the gain value(s) G_{i0} at the cavity entrance

$$G_{i0}(0, y) = G_{i0} = \text{const}, \tag{9}$$

and interrelating the incident and reflected light intensities at the cavity mirror surfaces

$$R^{+} N_{fi}^{+}(x, L_y) = N_{fi}^{-}(x, L_y), \tag{10}$$

$$R^{-} N_{fi}^{-}(x, 0) = N_{fi}^{+}(x, 0). \tag{11}$$

In Equations (1)–(8), the $N_m(J_i)$ and $N_n(J_i')$ indicate the populations of the upper (m, J_i) and lower (n, J_i') laser levels, respectively. N_m and N_n denote the populations of vibrational levels m and n, respectively. $\bar{B}_{nm}(J_i, J_i')$ and $\bar{B}_{mn}(J_i, J_i')$ are modified Einstein coefficients of the stimulated absorption and emission associated with radiative transfer $(m, J_i) \leftrightarrow (n, J_i')$ [5], [6]. Γ_{mi} and Γ_{ni} represent all energy exchange and relaxation source functions relevant to (m, J_i) and (n, J_i') levels, respectively. x and y are the Cartesian coordinates measuring the distance along the flow (x) and optical (y) axes, respectively (see Fig. 1). N_{fi}^{-} and N_{fi}^{+} describe the radiation field of the frequency ν_i within the cavity as expressed by the photon density moving back (N_{fi}^{-}) and forth (N_{fi}^{+}) between the mirrors Z^{-} and Z^{+} (see Fig. 1).

The coefficients $\bar{\beta}_i$ and $\bar{\theta}_{ij}$ are those defined in [4], and properly modified [5] to account for different notations used hereby and in [4]. For the application to Eqs. (7) and (8) the above mentioned coefficients follow the formulae:

$$\bar{\beta}_i = \frac{3}{8\pi} \frac{\gamma_{mn}}{\gamma} \frac{\nu^2 |R_{mn}|^4 \bar{N} \mathscr{L}^2(\omega - \nu_i)}{\varepsilon_0^2 \hbar^2 \gamma_m \gamma_n}, \tag{12}$$

$$\bar{\theta}_{ij} = \frac{1}{3} \bar{\beta}_i \left[2 + \frac{N_{2(i-j)}}{\bar{N}} \right] \left[\mathscr{L}(\omega - \nu_i) \mathscr{L}(\omega - \nu_j) + \mathrm{Re} \left\{ \frac{\gamma_m \gamma_n \gamma^2}{2(\gamma_m + \gamma_n)} \mathscr{D}(\omega - \nu_i) [\mathscr{D}_m(\nu_j - \nu_i) + \mathscr{D}_n(\nu_j - \nu_i)] [\mathscr{D}(\omega - \nu_i) + \mathscr{D}(\nu_j - \omega)] \right\} \right]. \tag{13}$$

In Equations (12) and (13) $\mathscr{D}_\alpha(\Delta\omega) = (\gamma_\alpha + i\Delta\omega)^{-1}$ is the complex frequency denominator ($\alpha = m, n$, or blank). $\mathscr{L}(\omega - \nu_i) = \dfrac{\gamma^2}{\gamma^2 + (\omega - \nu_i)^2}$ stands for the dimensionless Lorentzian. $|R_{mn}|$ denotes the electric dipole matrix element calculated for transfer between m and n levels. γ_m and γ_n are the upper and lower laser level decay constants, respectively. $\gamma_{mn} = \dfrac{1}{2}(\gamma_m + \gamma_n)$ describes the spontaneous emission and inelastic collisions contribution to the decay of the dipole. $\gamma = \gamma_{mn} + \gamma_{ph}$ indicates the dipole decay constant (γ_{ph} denotes the elastic collisions contribution to the dipole decay). ε_0 is the permittivity of vacuum; $\bar{N}$ is the average population inversion density, i.e., $\bar{N} = (1/L_y) \int_0^{L_y} N(y)\, dy$. $N_{2(i-j)}$ is the $2(j-i)$ Fourier component of the population inversion density, i.e., $N_{2(i-j)} = (1/L_y) \int_0^{L_y} N(y) \cos\left\{ \left[2(i-j) \dfrac{\pi}{L_y} \right] y \right\} dy$.

In what follows, it is assumed that the coefficients $\bar{\beta}_i$ and $\bar{\theta}_{ij}(\bar{\theta}_{ii} = \bar{\beta}_i)$ remain constant and that their values correspond to the state of the medium optical excitation at the cavity inlet cross-section ($x = 0$).

Equations (6)–(8) do not allow an analytical solution due to the nonlinear terms appearing on the right-hand sides of Eqs. (7) and (8). The possible use of the perturbation method has been disregarded, as for the expected high values of the radiation field intensity the changes in the cavity operation due to the line saturation phenomena should be expected to be of the same order as the first-order solution obtained under assumption that above effects can be neglected. To remove the mentioned square terms it is assumed that they can be approximated by the following formulae:

$$\bar{\beta}_i(N_{fi}^+)^2 + \sum_{j=i} \bar{\theta}_{ij} N_{fi}^+ N_{fj}^+ \simeq N_{fi}^+ [\bar{\beta}_i(N_{fi}^+)_s + \sum_{j \neq i} \bar{\theta}_{ij}(N_{fj}^+)_s],$$

$$\bar{\beta}_i(N_{fi}^-)^2 + \sum_{j \neq i} \bar{\theta}_{ij} N_{fi}^- N_{fj}^- \simeq N_{fi}^- [\bar{\beta}_i(N_{fi}^-)_s + \sum_{j \neq i} \bar{\theta}_{ij}(N_{fj}^-)_s]$$

where the steady-state photon densities $(N_{fi}^+)_s$ and $(N_{fi}^-)_s$ represent the solutions of the system of algebraic equations

$$c\bar{G}_i = \bar{\beta}_i(N_{fi}^+)_s + \sum_{j \neq i} \bar{\theta}_{ij}(N_{fj}^+)_s = \bar{\beta}_i(N_{fi}^-)_s + \sum_{j \neq i} \bar{\theta}_{ij}(N_{fj}^-)_s \tag{14}$$

written for some unspecified average value of the gain(s) closed between bounds defined by its maximum attainable value G_{i0} and its saturated value (common for all lines) $(1/L_y)\ln(1/\sqrt{R^+ R^-})$. Equation (15) shows that $(N_{fi}^+)_s = (N_{fi}^-)_s$. In what follows these quantities will be denoted as N_{si}. Further it is proposed to use as N_{si} the averaged value of the i-th line intensity sustained within the cavity operating under the assumption that the line saturation effects are negligible.

The assumptions summarized by Equation (14) permit us to rewrite Eqs. (7) and (8) in the forms:

$$\frac{\partial N_{fi}^+}{\partial y} = (G_i - \bar{G}_i) N_{fi}^+, \tag{15}$$

$$\frac{\partial N_{fi}^-}{\partial y} = -(G_i - \bar{G}_i) N_{fi}^-. \tag{16}$$

The starting set of equations and boundary conditions proposed for considering the multi-line cavity operation are thus composed of Eq. (6), Eqs. (15) and (16) and Eqs. (9)–(11).

3.2. Dimensionless equations, boundary conditions and notations

In appears convenient to rewrite Equations (6), (15) and (16) together with boundary conditions (9)–(11) in dimensionless forms [1], [5]. Choosing the scale of the photon number densities N_{fi}^+ and N_{fi}^- as equal to the population of the upper vibrational

laser level at the cavity entrance $N_{m0}(n_{fi}^{+} = N_{fi}^{+}/N_{m0}, \quad \bar{n}_{fi} = N_{fi}^{-}/N_{m0})$ and scaling the x and y by L_x and L_y, respectively ($\xi = x/L_x; \quad \eta = y/L_y$) one obtains:

$$\frac{\partial g_i}{\partial \xi} = -\Pi_{ci}[g_i(n_{fi}^{+}+n_{fi}^{-}) + \sum_{j \neq i} g_j(n_{fj}^{+}+n_{fj}^{-})], \tag{17}$$

$$\frac{\partial \ln n_{fi}^{+}}{\partial \eta} = -\frac{\partial \ln n_{fi}^{-}}{\partial \eta} = g_i - \bar{g}_i, \tag{18}$$

$$\bar{g}_i = \Pi_s(i,i) n_{si} + \sum_{j \neq i} \Pi_s(i,j) n_{sj}, \tag{19}$$

$$g_i(0,\eta) = \Pi_{vi} = (I_0 - \min I_{ti}) \frac{c^2 L_y A_{mn}}{8\pi v_i^2} N_{n0} f_m(T_0, J_i) \mathscr{L}(v, v_i), \tag{20}$$

$$R^{-} n_{fi}^{-}(\xi, 0) = n_{fi}^{+}(\xi, 0), \tag{21}$$

$$R^{+} n_{fi}^{+}(\xi, 1) = n_{fi}^{-}(\xi, 1). \tag{22}$$

In Equations (17)–(20) g_i and Π_{ci} denote the dimensionless gain assigned to the i-th line and the characteristic factor measuring the influence of the transverse flow-forced convection. They are given by the formulae:

$$g_i = \left[I_0 n_m(\xi,\eta) - \frac{g_{mi} f_n(T_0, J_i')}{g_{ni} f_m(T_0, J_i)} \bar{n}_n(\xi,\eta) \right] \frac{c^2 L_y A_{mn}(J_i, J_i')}{8\pi v_i^2} \times N_{n0} f_m(T_0, J_i) \mathscr{L}(v, v_i), \tag{23}$$

$$\Pi_{ci} = \frac{c}{v_0} \left[1 + \frac{g_{mi} f_n(T_0, J_i')}{g_{ni} f_m(T_0, J_i)} \right] \frac{c^2 L_x A_{mn}(J_i, J_i')}{8\pi v_i^2} N_{m0} f_m(T_0, J_i) \mathscr{L}(v, v_i). \tag{24}$$

In above, g_{mi} and g_{ni} indicate the statistical weights of the upper and lower laser level, respectively; $A_{mn}(J_i, J_i')$ stands for the Einstein coefficient of the spontaneous emission; $\mathscr{L}(v, v_i)$ denotes the normalized line shape-function. The dimensionless populations of the upper and lower vibrational laser level n_m and n_n entering Eq. (23), population inversion measure I_0 and its threshold value $\min I_{ti}$ (calculated for a lossless cavity), are defined by the following relations:

$$n_m(\xi,\eta) = N_m/N_{m0} = \exp\left\{ \frac{\hbar \omega_m}{k} \left[\frac{1}{T_{m0}} - \frac{1}{T_m(\xi,\eta)} \right] \right\},$$

$$n_n(\xi,\eta) = N_n/N_{n0} = \exp\left\{ \frac{\hbar \omega_n}{k} \left[\frac{1}{T_{n0}} - \frac{1}{T_n(\xi,\eta)} \right] \right\},$$

$$I_0 = N_{m0}/N_{n0} = \exp\left[\frac{\hbar}{k} \left(\frac{\omega_n}{T_{n0}} - \frac{\omega_m}{T_{m0}} \right) \right],$$

$$\min I_{ti} = \frac{\bar{B}_{nm}(J_i, J_i') f_n(T_0, J_i')}{\bar{B}_{mn}(J_i, J_i') f_m(T_0, J_i)} = \frac{g_{mi} f_n(T_0, J_i')}{g_{ni} f_m(T_0, J_i)} \lesssim 1$$

where $\hbar\omega_m/k$ and $\hbar\omega_n/k$ are the reference temperatures of the upper and lower vibrational laser level, respectively.

The i-th attenuation due to self- and cross-saturation processes enters Eqs. (18) via constant "gain(s)" $\bar{g}_i$ defined by relation (19). The parameters $\Pi_s(i,i)$ and $\Pi_s(i,j)$ represent there the self- and cross-line saturation coefficients (12) and (13) rewritten in dimensionless form, i.e.:

$$\Pi_s(ii) = 3\pi \frac{\gamma_{mn}}{\gamma^2} \frac{v^2 |R_{mn}|^4 \bar{N} N_{m0} L_y}{c\,\varepsilon_0^2 \hbar^2 \gamma_m \gamma_n} \mathscr{L}^2(\omega - v_i), \tag{25}$$

$$\begin{aligned} \Pi_s(i,j) = {} & \frac{\gamma_{mn}}{\gamma^2} \frac{v^2 |R_{mn}|^4 \bar{N} N_{m0} L_y}{c\,\varepsilon_0^2 \hbar^2 \gamma_m} \left[2 + \frac{N_{2(i-j)}}{\bar{N}} \right] \mathscr{L}^2(\omega - v_i) \\ & \times \left\{ \mathscr{L}(\omega - v_i)\, \mathscr{L}(\omega - v_j) + \mathrm{Re} \left\{ \frac{\gamma_m \gamma_n \gamma^2}{2(\gamma_m + \gamma_n)} \mathscr{D}(\omega - v_i) [\mathscr{D}_m(v_j - v_i) \right. \right. \\ & \left. \left. + \mathscr{D}_n(v_j - v_i)] [\mathscr{D}(\omega - v_i) + \mathscr{D}(v_j - \omega)] \right\} \right\}. \end{aligned} \tag{26}$$

The steady-state solution for each line intensity n_{si} is, according to the previously formulated assumption, given by relation

$$n_{si} \simeq \frac{1}{2} \int_0^1 [\bar{n}_{fi}^+(\xi, 1) + \bar{n}_{fi}^-(\xi, 1) - \bar{n}_{fi}^+(\xi, 0) + \bar{n}_{fi}^-(\xi, 0)] d\xi$$

where $n_{fi}^{+,-}(\xi, \eta_\alpha)(\eta_\alpha = 0,\ 1)$ represent the solutions of Eqs. (17), (18), (20)–(22) obtained for $\bar{g}_i \equiv 0$ [1]. Using relations quoted in [1], the above relation can be rewritten in the following form:

$$n_{si} \simeq \frac{1}{8} [(1 + R^+) \| \bar{n}_{fi}^+(\xi, 1) \| + (1 + R^-) \| \bar{n}_{fi}^-(\xi, 0) \|] \tag{27}$$

where the norms $\| \bar{n}_{fi}^+(\xi, 1) \|$ and $\| \bar{n}_{fi}^-(\xi, 0) \|$ of $\bar{n}_{fi}^+(\xi, 1)$ and $\bar{n}_{fi}^-(\xi, 0)$ Dirac's pseudo-functions $\delta_D(\xi)$ are given by the following formulae [1]:

$$\begin{aligned} \| \bar{n}_{fi}^+(\xi, 1) \| = {} & \left\{ \ln \left[\frac{\exp(-\Pi_{vi}) - x_{1i}^+(0)}{\exp(-\Pi_{vi}) - x_{2i}^+(0)} \frac{x_{2i}^+(0) - \sqrt{R^+ R^-}}{x_{1i}^+(0) - \sqrt{R^+ R^-}} \right] \right\} \\ & \times \left\{ \frac{1}{2} \Pi_{ci} \Phi_{ji}^+(0) [x_{1i}^+(0) - x_{2i}^+(0)] \right\}^{-1}, \end{aligned} \tag{28}$$

$$\begin{aligned} \| \bar{n}_{fi}^-(\xi, 0) \| = {} & \left\{ \ln \left[\frac{\exp(-\Pi_{vi}) - x_{1i}^-(1)}{\exp(-\Pi_{vi}) - x_{2i}^-(1)} \frac{x_{2i}^-(1) - \sqrt{R^+ R^-}}{x_{1i}^-(1) - \sqrt{R^+ R^-}} \right] \right\} \\ & \times \left\{ \frac{1}{2} \Pi_{ci} \Phi_{ji}^-(1) [x_{1i}^-(1) - x_{2i}^-(1)] \right\}^{-1}. \end{aligned} \tag{29}$$

In Equations (26) and (27) $x_{1i}^+(\eta)$, $x_{2i}^+(\eta)$, $x_{1i}^-(\eta)$ and $x_{2i}^-(\eta)$ are roots of two following equations:

$$x^2\,\Phi_{ji}^{+}(\eta)-[\Phi_{ji}^{+}(1)-R^{+}\,\Psi_{ji}^{+}(1)]\,x-R^{+}\,\Psi_{ji}^{+}(\eta)=0,$$

$$x^2\,\Phi_{ji}^{-}(\eta)-[\Phi_{ji}^{-}(0)-R^{-}\,\Psi_{ji}^{-}(0)]\,x-R^{-}\,\Psi_{ji}^{-}(\eta)=0$$

where the auxiliary functions $\Phi_{ji}^{+,-}(\eta)$ and $\Psi_{ji}^{+,-}(\eta)$ are defined as equal to:

$$\Phi_{ji}^{+}(\eta)=1+\sum_{j\neq 1}^{\prime}\frac{f_m(T_0,J_j)\,\mathscr{L}(\nu,\nu_i)}{f_m(T_0,J_i)\,\mathscr{L}(\nu,\nu_j)}\exp[-(\Pi_{vi}-\Pi_{vj})(\eta-1)],$$

$$\Psi_{ji}^{+}(\eta)=1+\sum_{j\neq 1}\frac{f_m(T_0,J_j)\,\mathscr{L}(\nu,\nu_i)}{f_m(T_0,J_i)\,\mathscr{L}(\nu,\nu_j}\exp[-(\Pi_{vj}-\Pi_{vi})\eta],$$

$$\Phi_{ji}^{-}(\eta)\equiv\Psi_{ji}^{+}(\eta),\quad \Psi_{ji}^{-}(\eta)\equiv\Phi_{ji}^{+}(\eta).$$

The norms $\|\bar{n}_{fi}^{+}(\xi,1)\|$ and/or $\|\bar{n}_{fi}^{-}(\xi,0)\|$ differ from zero in the whole range of the cavity losses (measured by $\sqrt{R^{+}R^{-}}$) in which the following inequality is satisfied [1]

$$\exp(-\Pi_{vi})<\sqrt{R^{+}R^{-}}<x_{1i}^{+}(0)\equiv x_{1i}^{-}(1)=1+\sum_{j\neq i}\frac{f_m(T_0,J_j)\,\mathscr{L}(\nu,\nu_i)}{f_m(T_0,J_i)\,\mathscr{L}(\nu,\nu_j)}\exp[-(\Pi_{vj}-\Pi_{vi})].$$

The lower admissible bound of the $\sqrt{R^{+}R^{-}}$ values is due to the requirement that any given line can be sustained in the cavity only if its gain exceeds the cavity losses. The upper bound limit of the admissible $\sqrt{R^{+}R^{-}}$ values results from the fact that with the increasing number of lines (increase in $\sqrt{R^{+}R^{-}}$) the first (high gain) lines are being switched-off transmitting their energy into sustaining the Maxwellian form of the rotational energy distribution function [1]. For each $\sqrt{R^{+}R^{-}}$ satisfying the last inequality the line saturation effects will appear in Eqs. (17)–(22) ($\bar{g}_i>0$) affecting the power characteristics of the resonator under description.

3.3. Formal solutions

The dimensionless equations had been reduced to Equations (17)–(22).

Introducing abbreviated notations:

$$A_{fi}^{+}(\xi,\eta_\alpha/\eta_\beta)=n_{fi}^{+}(\xi,\eta_\alpha)/n_{fi}^{+}(\xi,\eta_\beta),\quad A_{fi}^{-}(\xi,\eta_\alpha/\eta_\beta)=n_{fi}^{-}(\xi,\eta_\alpha)/n_{fi}^{-}(\xi,\eta_\beta),$$

$$A_{fj,i}^{+}(\xi,\eta_\alpha/\eta_\beta)=n_{fj}^{+}(\xi,\eta_\alpha)/n_{fi}^{+}(\xi,\eta_\alpha),\quad A_{fj,i}^{-}(\xi,\eta_\alpha/\eta_\beta)=n_{fj}^{-}(\xi,\eta_\alpha)/n_{fi}^{-}(\xi,\eta_\beta),$$

one obtains immediately from Eqs. (18), (21) and (22):

$$A_{fi}^{+}(\xi,\eta/0)=\exp\left[\left(\int_0^{\eta}g_i(\xi,\eta)\,d\eta\right)-\bar{g}_i\eta\right], \tag{30}$$

$$A_{fi}^{-}(\xi,\eta/0)=[A_{fi}^{+}(\xi,\eta/0)]^{-1}, \tag{31}$$

$$A_{fi}^{+}(\xi,\eta/0)\,A_{fi}^{-}(\xi,\eta/0)=A_{fi}^{+}(\xi,1/\eta)\,A_{fi}^{-}(\xi,1/\eta), \tag{32}$$

$$A_{fi}^{+}(\xi,1/0)=A_{fi}^{-}(\xi,0/1)=\sqrt{R^{+}R^{-}}. \tag{33}$$

The last relation states the conditions under which the i-th line radiation field can be self-reproducing upon the surfaces of the resonator mirrors [1], [7]. Furthermore,

Eq. (31) indicates that the photon densities assigned to all lines under consideration will be, as in [1], given by normalized Dirac's delta-pseudo functions, i.e., [7]

$$n^{+}_{fi}(\xi,\eta) = \|n^{+}_{fi}(\eta)\|\,\delta_{\mathrm{D}}(\xi), \quad n^{-}_{fi}(\xi,\eta) = \|n^{-}_{fi}(\eta)\|\,\delta_{\mathrm{D}}(\xi).$$

Based upon Eqs. (20) and (30) one can recover the following approximate formulae for ratio(s) of the i-th and j-th line photon number densities [1]:

$$A^{-}_{fj,i}(\xi,\eta/\eta) \simeq \frac{f_m(T_0,J_j)\,\mathscr{L}(\nu,\nu_i)}{f_m(T_0,J_i)\,\mathscr{L}(\nu,\nu_j)} \exp\left[-(\Pi_{vj}-\Pi_{vi}+\bar{g}_i-\bar{g}_j)\,\eta\right], \tag{34}$$

$$A^{+}_{fj,i}(\xi,\eta/\eta) \simeq \frac{f_m(T_0,J_j)\,\mathscr{L}(\nu,\nu_i)}{f_m(T_0,J_i)\,\mathscr{L}(\nu,\nu_j)} \exp\left[-(\Pi_{vj}-\Pi_{vi}+\bar{g}_i-\bar{g}_j)(1-\eta)\right]. \tag{35}$$

To determine the unknown norms entering the formal solutions (32) and (33) Eqs. (17) and (18) ought to be integrated. By recovering g_i and $g_i n^{+,-}_{fi}$ from Eqs. (17) and introducing them into Eq. (18) the following two equations can be obtained:

$$\frac{\partial}{\partial\eta}\Bigg[-\frac{1}{\Pi_{ci}}\frac{\partial \ln n^{+}_{fi}}{\partial\xi} - n^{+}_{fi} + n^{-}_{fi} - \sum_{j\neq i}(n^{+}_{fi}-n^{-}_{fj}) - \bar{g}_i\int_1^{\eta}(n^{+}_{fi}+n^{-}_{fi})\,d\eta - \sum_{j\neq i}\bar{g}_j\int_1^{\eta}(n^{+}_{fj}+n^{-}_{fj})\,d\eta\Bigg] = 0, \tag{36}$$

$$\frac{\partial}{\partial\eta}\Bigg[-\frac{1}{\Pi_{ci}}\frac{\partial \ln n^{-}_{fi}}{\partial\eta} - n^{+}_{fi} + n^{-}_{fi} - \sum_{j\neq i}(n^{+}_{fj}-n^{-}_{fj}) - \bar{g}_i\int_1^{\eta}(n^{+}_{fi}+n^{-}_{fi})\,d\eta - \sum_{j\neq i}\bar{g}_j\int_1^{\eta}(n^{+}_{fj}+n^{-}_{fj})\,d\eta\Bigg] = 0. \tag{37}$$

Assuming that:

$$\int_1^{\eta}[n^{+}_{fi}(\xi,\eta)+n^{-}_{fi}(\xi,\eta)]\,d\eta \simeq \frac{\eta-1}{2}[n^{+}_{fi}(\xi,\eta)+n^{+}_{fi}(\xi,1)+n^{-}_{fi}(\xi,\eta)+n^{-}_{fi}(\xi,1)],$$

$$\int_0^{\eta}[n^{+}_{fi}(\xi,\eta)+n^{-}_{fi}(\xi,\eta)]\,d\eta \simeq \frac{\eta}{2}[n^{+}_{fi}(\xi,\eta)+n^{+}_{fi}(\xi,0)+n^{-}_{fi}(\xi,\eta)+n^{-}_{fi}(\xi,0)],$$

and making use of relations (21), (22), (34) and (35), Eqs. (36) and (37) can be transformed into the following Bernoulli equations:

$$-\frac{1}{\Pi_{ci}}\frac{dA^{+}_{fi}(\xi,\eta/1)}{d\xi} = \Phi^{+}_{1i}(\eta)\,n^{+}_{fi}(\xi,1)\,[A^{+}_{fi}(\xi,\eta/1)-x^{+}_{1i}(\eta)]\,[A^{+}_{fi}(\xi,\eta/1)-x^{+}_{2i}(\eta)], \tag{38}$$

$$-\frac{1}{\Pi_{ci}}\frac{dA^{-}_{fi}(\xi,\eta/0)}{d\xi} = \Phi^{-}_{1i}(\eta)\,n^{-}_{fi}(\xi,0)\,[A^{-}_{fi}(\xi,\eta/0)-x^{-}_{1i}(\eta)]\,[A^{-}_{fi}(\xi,\eta/0)-x^{-}_{2i}(\eta)]. \tag{39}$$

In Equations (38) and (39) $x^{+,-}_{1i}$ and $x^{+,-}_{2i}$ denote the roots of algebraic equations:

$$x^2\,\Phi^{+}_{1i}(\eta) - x\,\Phi^{+}_{2i}(\eta) - \Phi^{+}_{3i}(\eta) = 0, \tag{40}$$

$$x^2\,\Phi^{-}_{1i}(\eta) - x\,\Phi^{-}_{2i}(\eta) - \Phi^{-}_{3i}(\eta) = 0, \tag{41}$$

in which the functions $\Phi_{ki}^{+,-}$ $(k = 1, 2, 3)$ are given by the following relations:

$$\Phi_{1i}^{+}(\eta) = 1-\frac{\bar{g}_i(1-\eta)}{2}+\sum_{j\neq i}\left[1-\frac{\bar{g}_j(1-\eta)}{2}\right]A_{fj,i}^{+}(\xi,\eta/\eta), \tag{42}$$

$$\Phi_{2i}^{+}(\eta) = 1-R^{+}+(1+R^{+})\frac{\bar{g}_i(1-\eta)}{2}+\sum_{j\neq i}\left\{[A_{fj,i}^{+}(\xi,1/1)-R^{+}A_{fj,i}^{-}(\xi,1/1)]\right.$$
$$\left.+\frac{\bar{g}_i(1-\eta)}{2}[A_{fj,i}^{+}(\xi,1/1)+R^{+}A_{fj,i}^{-}(\xi,1/1)]\right\}, \tag{43}$$

$$\Phi_{3i}^{+}(\eta) = R^{+}\left\{\left[1+\frac{\bar{g}_i(1-\eta)}{2}\right]+\sum_{j\neq i}\left[1+\frac{\bar{g}_j(1-\eta)}{2}\right]A_{fj,i}^{-}(\xi,\eta/\eta)\right\}, \tag{44}$$

$$\Phi_{1i}^{-}(\eta) = 1-\frac{\bar{g}_i\eta}{2}+\sum_{j\neq i}\left[1-\frac{\bar{g}_j\eta}{2}\right]A_{fj,i}^{-}(\xi,\eta/\eta), \tag{45}$$

$$\Phi_{2i}^{-}(\eta) = 1-R^{-}+(1+R^{-})\frac{\bar{g}_i\eta}{2}+\sum_{j\neq i}\left\{[A_{fj,i}^{-}(\xi,0/0)-R^{-}A_{fj,i}^{+}(\xi,0/0)]\right.$$
$$\left.+\frac{\bar{g}_j\eta}{2}[A_{fj,i}^{-}(\xi,0/0)+R^{-}A_{fj,i}^{+}(\xi,0/0)]\right\}, \tag{46}$$

$$\Phi_{3i}^{-}(\eta) = R^{-}\left[\left(1+\frac{\bar{g}_i\eta}{2}\right)+\sum_{j\neq i}\left(1+\frac{\bar{g}_j\eta}{2}\right)A_{fj,i}^{+}(\xi,\eta/\eta)\right]. \tag{47}$$

The solution of Equation (38) should be sought for together with boundary condition

$$A_{fi}^{+}(0,\eta/1) = \exp[-(\Pi_{vi}-\bar{g}_i)(1-\eta)]. \tag{48}$$

The integral trajectory of Eq. (39) passes (for $\xi = 0$) through the point

$$A_{fi}^{-}(0,\eta/0) = \exp[-(\Pi_{vi}-\bar{g}_i)\eta]. \tag{49}$$

Solving Equations (38) and (39) with the above given boundary conditions, and employing the general relation (31), one obtains the formulae defining the sought for norms of photon number density distributions over the $\mathbf{Z}^{+}$ and $\mathbf{Z}^{-}$ mirror surfaces

$$||n_{fi}^{+}(\xi,1)|| = \left[\left[\ln\left\{\frac{\exp[-(\Pi_{vi}-\bar{g}_i)]-x_{1i}^{+}(0)}{\exp[-(\Pi_{vi}-\bar{g}_i)]-x_{2i}^{+}(0)}\frac{x_{2i}^{+}(0)-\sqrt{R^{+}R^{-}}}{x_{1i}^{+}(0)-\sqrt{R^{+}R^{-}}}\right\}\right]\right]$$
$$\times\left\{\frac{1}{2}\Pi_{ci}\Phi_{1i}^{+}(0)[x_{1i}^{+}(0)-x_{2i}^{+}(0)]\right\}^{-1}, \tag{50}$$

$$||n_{fi}^{-}(\xi,0)|| = \left[\left[\ln\left\{\frac{\exp[-(\Pi_{vi}-\bar{g}_i)]-x_{1i}^{-}(1)}{\exp[-(\Pi_{vi}-\bar{g}_i)]-x_{2i}^{-}(1)}\frac{x_{2i}^{-}(1)-\sqrt{R^{+}R^{-}}}{x_{1i}^{-}(1)-\sqrt{R^{+}R^{-}}}\right\}\right]\right]$$
$$\times\left\{\frac{1}{2}\Pi_{ci}\Phi_{1i}^{-}(1)[x_{1i}^{-}(1)-x_{2i}^{-}(1)]\right\}^{-1}. \tag{51}$$

By comparing Equations (40), (42)–(44) with Eqs. (41), (45)–(47), it can be seen that the norm (50) equals (51) after the position of the resonator mirrors $R^+ \leftrightarrow R^-$ is reversed. In paper [1], it was suggested that this, though somewhat trivial observation, can be nevertheless regarded as a proof of physical consistency of the hitherto reported formal results. The relations (50) and (51) being known the problem can be considered as formally closed. These formulae permit us to calculate any output power characteristic of the multiline CW-GDL cavity.

3.4. Main power characteristics

The single line output power p_{fi}, total net laser output $p_f = \sum_i p_{fi}$, load coefficients (efficiencies) of the output beam composite lines $\mathfrak{k}_{fi}$ and the cavity overall efficiency $\eta_f = \sum_i \mathfrak{k}_{fi}$ can be all expressed through a dimensionless single-line output power measure $\overline{p_{fi}(\mathbf{G})}$ and through virtual radiation power P_v at the cavity inlet boundary. The last quantity is identified with the available power brought to the cavity entrance with the transverse flow of the molecules excited to the upper (m) vibrational laser level. It is therefore given by following relation

$$P_v = \frac{1}{2} h v_0 L_y L_z N_{m0} \sum_i v_i f_m(T_0, J_i) = h v_0 L_y L_z N_{m0} \langle v_i \rangle \tag{52}$$

where $\langle v_i \rangle$ defines the mean frequency of the virtual radiation field calculated by weighing the single-line $(m, J_i) \leftrightarrow (n, J_i')$ central frequencies v_i by the corresponding values of the Maxwell-Boltzman distribution function $f_m(T_0, J_i)$. In paper [1] it was shown that – to good degree of approximation – $\langle v_i \rangle$ equals $v_{mn} + Bc$ where v_{mn} defines the band origin. The single-line dimensionless output power measure is defined by the following formula

$$\overline{p_{fi}(\mathbf{G})} = \frac{1}{2} \frac{v_i}{\langle v_i \rangle} [(1 - R^+) ||n_{fi}^+(\xi, 1)|| + (1 - R^-) ||n_{fi}^-(\xi, 0)||]. \tag{53}$$

It is proportional to the number of photons leaving the cavity region through both semi-transparent mirrors. In view of solutions (50) and (51) the relation (53) can be rewritten in the following form:

$$\overline{p_{fi}(\mathbf{G})} = \left\{ \frac{\exp[-(\Pi_{vi} - \bar{g}_i)] - x_{1i}^-(1)}{\exp[-(\Pi_{vi} - \bar{g}_i)] - x_{2i}^-(1)} \frac{x_{2i}^-(1) - \sqrt{R^+ R^-}}{x_{1i}^-(1) - \sqrt{R^+ R^-}} \right\}^{\alpha}$$
$$\times \left\{ \frac{\exp[-(\Pi_{vi} - \bar{g}_i)] - x_{1i}^+(0)}{\exp[-(\Pi_{vi} - \bar{g}_i)] - x_{2i}^+(0)} \frac{x_{2i}^+(0) - \sqrt{R^+ R^-}}{x_{1i}^+(0) - \sqrt{R^+ R^-}} \right\}^{\beta} \tag{54}$$

where the exponents α and β are given by the formulae:

$$\alpha = \frac{1}{\Pi_{ci}} \frac{v_i}{\langle v_i \rangle} \frac{1 - R^-}{\Phi_{1i}^-(1)[x_{1i}^-(1) - x_{2i}^-(1)]},$$

and

$$\beta = \frac{1}{\Pi_{ci}} \frac{\nu_i}{\langle \nu_i \rangle} \frac{1-R^+}{\Phi_{1i}^+(0)\,[x_{1i}^+(0)-x_{2i}^+(0)]},$$

respectively.

With P_v and $\overline{p_{fi}(\mathbf{G})}$ determined by Eqs. (52) and (54), the desired power characteristic(s) of the cw gasdynamic laser can be calculated by empolying the following expressions:

$$\mathfrak{k}_{fi}(\mathbf{G}) = \Pi_{ii}(\Pi_{ci}/\Pi_{vi}) \ln \overline{p_{fi}(\mathbf{G})}, \tag{55}$$

$$p_{fi} = \mathfrak{k}_{fi}(\mathbf{G}) P_v, \tag{56}$$

$$\eta_f(\mathbf{G}) = \sum_i \mathfrak{k}_{fi}(\mathbf{G}) = \ln \prod_i [\overline{p_{fi}(\mathbf{G})}]^{\Pi_{ii}\Pi_{ci}/\Pi_{vi}}, \tag{57}$$

$$p_f = \eta_f(\mathbf{G}) P_v. \tag{58}$$

The factor Π_{ii} appearing in Eqs. (55)–(58) defines the dimensionless measure of the partial (for i-th transition) population inversion. It satisfies the relation

$$\Pi_{ii} = \frac{1}{I_0} \frac{I_0 - \min I_{ti}}{1+\min I_{ti}} < \frac{1}{1+\min I_{ti}} \simeq \frac{1}{2} \simeq \lim_{I_0 \nearrow \infty} \Pi_{ii}. \tag{59}$$

This parameter describes the maximum value of the single-line efficiency which could be reached if the cavity under consideration worked in accordance with Lee's criterion of the global balance between the single-line gain and cavity losses [3], [7], [8].

The formulae presented so far are subject to the initial assumption that the flow-forced convection is a source of the vibrational energy far exceeding in strength both the collisional V–V pumping and V–T relaxation. Usually the CW-GDL contains the pumping medium and the catalyst to ensure the efficiency of both above mentioned processes. The upper attainable limit of CW-GDL output can be specified as that corresponding to an ideal case of total relaxation of the lower laser level ($n_n \searrow 0$, $I_0 \nearrow \infty$) and detailed equilibrium between m-level and close to it p-level of the pumping medium. In [1] it was suggested that the solution given by Eqs. (55)–(58) could be adapted to estimate the laser output power and efficiency in the above described ideal pumping and relaxation case if one substitutes the dimensionless parameters Π_{vi}, Π_{ci} and Π_{ii} are substituted by the new ones defined by the relations:

$$\Pi_{vi}^* = \Pi_{vi}(n_n \searrow 0, I_0 \nearrow \infty) = \frac{c^2 L_y A_{mn}(J_i, J_i') N_{m0} \mathscr{L}(\nu, \nu_i)}{8\pi \nu_i^2} > \Pi_{vi}, \tag{60}$$

$$\Pi_{ci}^* = \Pi_{ci}/(1+I_p) < \Pi_{ci}, \tag{61}$$

$$\Pi_{ii}^* = (1+\min I_{ti})^{-1} = \Pi_{ii}(I_0 \nearrow \infty) > \Pi_{ii}. \tag{62}$$

In the above relations I_p indicates the ratio of the number of molecules of the pumping medium excited to the p-vibrational level to the number of molecules of the lasing medium excited to the upper vibrational laser level, i.e.

$$I_p = (N_p/N_l)\exp\left[\frac{\hbar}{k}\left(\frac{\omega_m}{T_{m0}} - \frac{\omega_p}{T_{p0}}\right)\right] \tag{63}$$

where: N_p and N_l are the concentrations of the pumping and optically active medium, respectively; $\hbar\omega_p/k$ and T_{p0} stand for the reference temperature of the p-level and vibrational temperature of the pumping medium at the cavity entrance, respectively.

From Equation (54) and Equations (55)–(57) the usually encountered requirements can be recovered. They should be satisfied for each individual line to be sure that it will not be cut-off from the virtual spectrum due to too high or too low losses of the cavity. The exigency that $p_{fi} > 0$ is, in view of Eqs. (54)–(56), satisfied under the following three conditions:

$$I_0 > \min I_{ti} = \frac{2J_i+1}{2J_i'+1}\exp\left\{\frac{hcB}{kT_0}[J_i(J_i+1) - J_i'(J_i'+1)]\right\}, \tag{64}$$

$$\exp\{-[\Pi_{vi} - \Pi_s(i,i)n_{si} - \sum_{j\neq i}\Pi_s(i,j)n_{sj}\} < \sqrt{R^+R^-}, \tag{65}$$

$$\sqrt{R^+R^-} < x_{1i}^+(0) \equiv x_{1i}^-(1). \tag{66}$$

The first, somewhat trivial one results from the definition of the threshold value of the medium optical excitation at the cavity entrance and is always fulfilled if the more strident constraints of gain-cavity losses balance constraints (65) are satisfied. The last inequality (66) sets an upper admissible limit on the values of resonator mirror reflectivity coefficient. This limitation of $\sqrt{R^+R^-}$ value results from the fact that with decrease of the cavity losses the number of lines which appear and could be sustained, in accordance with the requirement (65), increases and the energy of the first lines is transmitted into sustaining the Maxwellian form of the rotational energy distribution function [1]. In the case under consideration the energy of lines also decreases via the line conversion (cross-saturation) process to eventually weaker lines are fed by the flux of energy coming from the lines of high gain value. It is evident from Eqs. (40), (47) and (65)–(66) that the line self- and cross-saturation processes narrow the region of the cavity losses in which each individual line could be generated and sustained if $\bar{g}_i$ was negligible. It should be mentioned that in what follows all lines will be ordered by decrease relation Π_{vi} and that 1-th line will therefore indicate that one for which the gain at the cavity entrance achieves its maximum; $J_1 = E[(kT/2B\hbar c) - 1/2]$, where $E(x)$ stands for the entire function of its own argument. It seems also to be worth noticing that for each chosen value of the cavity losses ($\sqrt{R^+R^-} = \text{const}$) the inequalities (65) and (66) define the maximum number of lines which can coexist within the optical resonator. The summation and

multiplication, indexed by line number i, is always extended only over the lines which can be simultaneously sustained in the cavity. The exception is made in the relation defining the virtual radiation power (se Eq. (52)), as the virtual spectrum is obviously not subject to constraints imposed by requirements (65) and (66). In a general case, the quantitative estimation of the influence of line self- and cross-saturation processes upon the cw multiline cavity operation cannot be easily carried out, since the number of free parameters $(\Pi_{vi}, \Pi_{ci}, \Pi_{ii}, \nu_i/\langle\nu_i\rangle; i = 1, 2, \ldots, k)$ is obviously too high.

The steady-state photon number density (scaled by N_{m0} (see Eqs. (25)–(27)) is lower than one. The dimensionless coefficients measuring the self- and cross-saturation effects are of the order of ten (see Eqs. (23) and (24)). It seems logical, therefore, to suppose that the quantitative influence of line saturation upon the laser performance will be more important for low gain lines appearing at lower cavity losses (for high $\sqrt{R^+ R^-}$) than for high gain lines excited at lower $\sqrt{R^+ R^-}$ values. With the increasing value of $\sqrt{R^+ R^-}$ not only the low gain lines will prevail in the spectrum of laser output beam, but also it should be expected that the value g_i will increase, and the line attenuation depending on the difference $\Pi_{vi} - \bar{g}_i$ will be more pronounced than for high $\Pi_{vj<i}$ and low $\bar{g}_{j<i}$ lines [1]. However, the relation (65) shows that with $\sqrt{R^+ R^-}$ increasing the high gain lines will be switched-off leading to drop of the $\bar{g}_i$ value. Summing-up, it can be stated that the answer to the question which lines will be most sensitive to the influence of the line saturation processes is not altogether simple and can be obtained only from pertinent numerical calculations.

A numerical example, given in the next Section of this paper, makes it possible to carry out the comparison between typical CW-GDL cavities operating under alternative assumptions that the line saturation phenomena can or cannot be neglected.

3.5. Numerical example concerning the cavity of a CO_2 CW-GDL

All parameters $[\Pi_{vi}, \Pi_{ci}, \Pi_{ii}, \Pi_s(ii), \Pi_s(i,j), \Pi_{si}, \nu_i/\langle\nu_i\rangle]$ influencing the multiline cavity power characteristics are determined on the basis of the medium optical excitation and flow parameters at the cavity inlet cross-section, which are related to the gas-mixture flow history within the CW-GDL channel region preceding the optical resonator. Thus, these parameters must be determined by solving a couplet system of gasdynamic equations and rate equations for vibrational energy exchange and relaxation. To allow a comparison with the cavity operating under conditions in which the line saturation effects can be neglected, the numerical example, quoted in this paper, will concern a CW-GDL driven by the benzene combustion in compressed air [1]. The numerical calculations have been described in detail in paper [1]. The values of coefficients $\nu_i/\langle\nu_i\rangle$, Π_{vi}, Π_{ci}, Π_{ii} are listed in Tables 1 and 2.

The basic results of the described calculations are summarized in Figs. 3 and 4, where the line saturation measure

Table 1. Values of characteristic parameters Π_{vi}, Π_{ci}, Π_{ii} and $v_i/\langle v_i \rangle$ for the case of negligible pumping and relaxation

i	Line	$v_i/\langle v_i \rangle$	Π_{vi}	$\Pi_{ci} \cdot 10^{-4}$	Π_{ii}
1	R (24)	1.0203	0.47714	1.0735	0.34743
2	R (26)	1.0222	0.47575	1.0801	0.34429
3	R (21)	1.0184	0.47065	1.0484	0.35091
4	R (28)	1.0242	0.46715	1.0695	0.34141
5	R (20)	1.0165	0.45580	1.0040	0.35484
6	P (20)	0.9775	0.45390	1.0155	0.34936
7	R (30)	1.0261	0.45222	1.0435	0.33874
8	P (22)	0.9753	0.45067	1.0025	0.38139
9	P (18)	0.9797	0.44960	1.0121	0.34721
10	P (24)	0.9731	0.44065	0.9748	0.35331
.					
.					
.					
.					
.					
.					
58	P (56)	0.9340	0.06093	0.1256	0.37901
59	R (62)	1.0613	0.05670	0.1441	0.30752
60	P (58)	0.9314	0.04933	0.1013	0.38049

Table 2. Modified values of characteristic parameters Π^*_{vi}, Π^*_{ci}, and Π^*_{ii} for the case of ideal pumping and relaxation

i	Π^*_{vi}	$\Pi^*_{ci} \cdot 10^{-3}$	Π^*_{ii}
1	0.69268	2.0777	0.50437
2	0.69366	2.0905	0.50199
3	0.68003	2.0291	0.50702
4	0.68389	2.0700	0.49980
5	0.65511	1.9433	0.51000
6	0.65720	1.9655	0.50584
7	0.66454	2.0197	0.49777
8	0.65074	1.9403	0.50738
9	0.65289	1.9589	0.50421
10	0.63462	1.8868	0.50889
.			
.			
.			
.			
.			
.			
58	0.08494	0.2432	0.52836
59	0.08740	0.2789	0.47406
60	0.06851	0.1961	0.52948

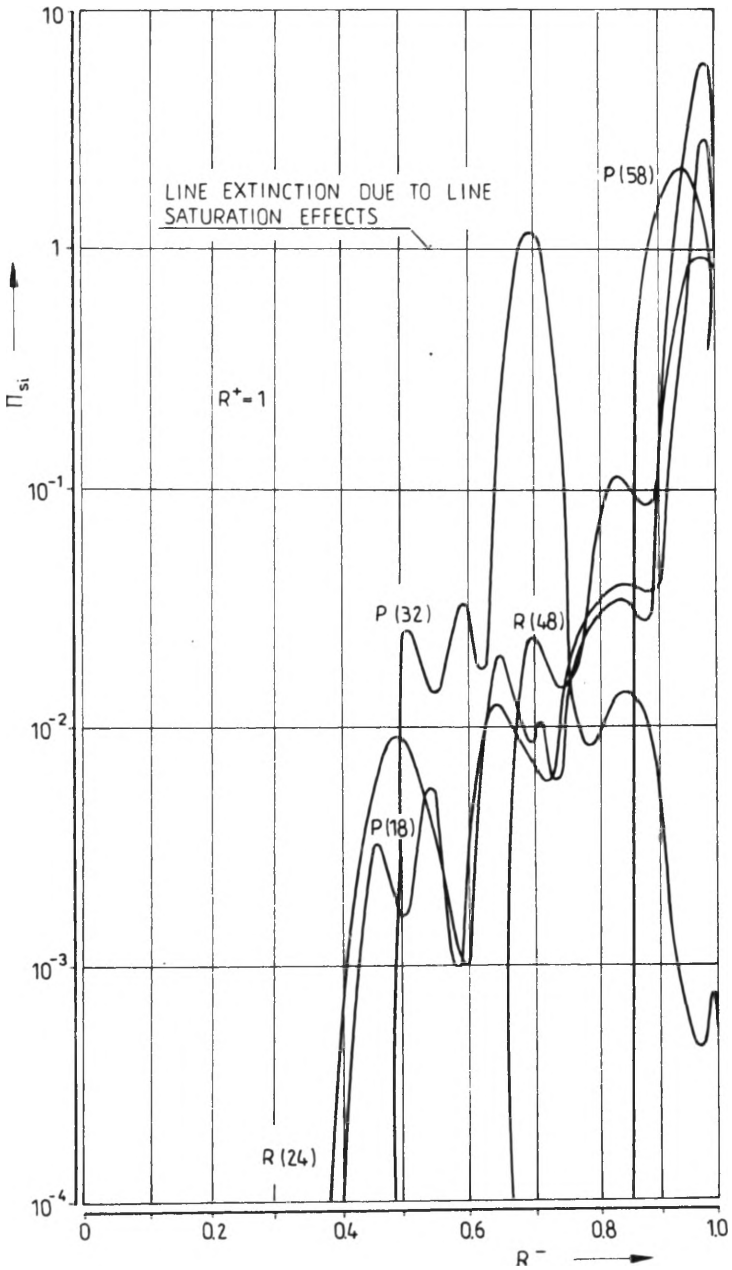

Fig. 3. Line attenuation coefficient Π_{si} for the case of negligible pumping and relaxation

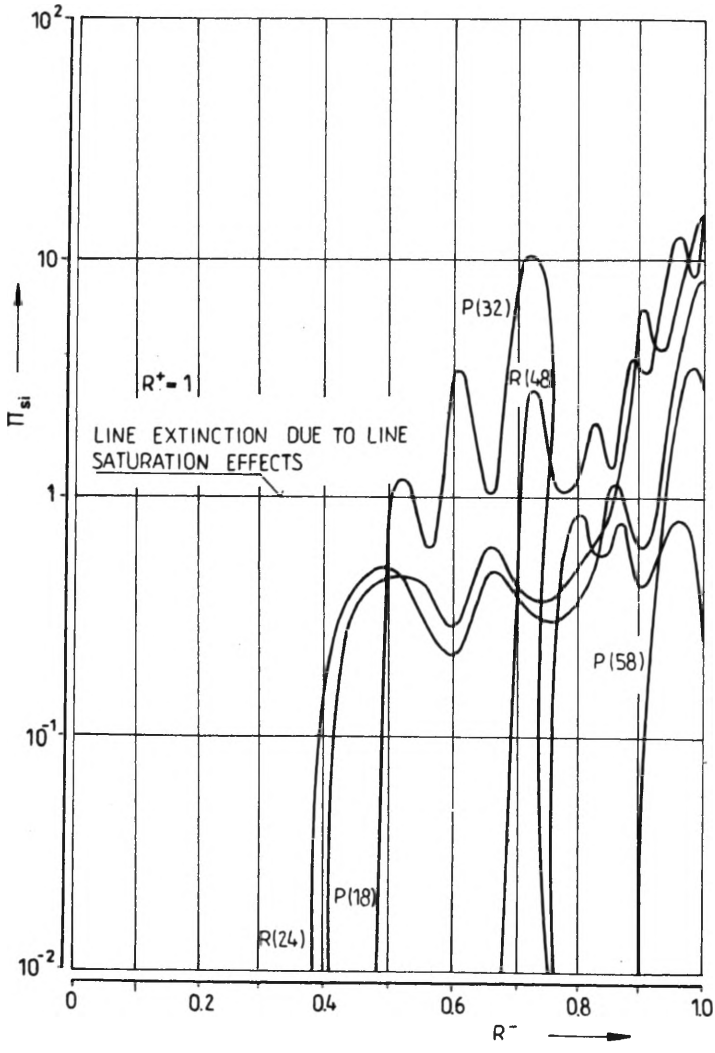

Fig. 4. Line attenuation coefficient Π_{si} for the case of ideal pumping and relaxation

$$\Pi_{si} = \Pi_{vi}^{-1}[\Pi_s(i,i)\, n_{si} + \sum_{j \neq i} \Pi_s(i,j)\, n_{sj}] \tag{67}$$

has been presented as function of the cavity absorption losses for various lines from the spectrum available at the cavity entrance; the calculations were carried out for 60 different lines. From Figures 3 and 4 it seems evident that the influence of line cross- and self-saturation becomes more important when the overall efficiency of laser power extraction increases, i.e., in the case of ideal pumping and relaxation. However, it has been shown in paper [5] that this influence is not very important from the technological point of view. These basically meaningful effects can be disregarded when estimating the expected output of CW-GDL treated purely as a device to convert the energy of the working gas mixture into radiation field energy.

4. Influence of transverse mode(s) on the multiline cw gas dynamic laser cavity operation

4.1. Additional assumptions and formal solutions

In the precedent considerations the cavity losses were evenly assigned to all the lines under consideration, i.e., it has been tacitly assumed that all considered lines pertain to the same single transverse mode of the radiation field distribution. It seems obvious that due to high values of the Fresnel number encountered in CW-GDL cavities and high values of gain which can be reached by means of the supersonic expansion, the CW-GDL resonators operate in the multi-transverse mode regime.

The quantitative description of these above operating conditions of CW-GDL multi-line cavity can be formulated by including the individual transverse mode diffractional losses into the mirror reflectivity coefficients, thus modifying the boundary conditions (10), (11) and (21), (22). By the same token each individual line (longitudinal mode) intensity ought to be split into the composite transverse mode intensities.

Neglecting the line saturation effects, i.e., putting everywhere $\bar{g}_i = 0$, the starting set of rate equations describing the performance of multi-line, multi-transverse mode cavity can be recovered by a direct adaptation of Eqs. (17) and (18), which takes the following forms:

$$\frac{\partial g_i}{\partial \xi} = - \Pi_{ci}[g_i(n_{fi}^{+}+n_{fi}^{-})+ \sum_{j \neq i} g_j(n_{fj}^{+}+n_{fj}^{-})], \tag{68}$$

$$n_{fi}^{+} = \sum_{m,n} n_{fi,m,n}^{+}, \quad n_{fi}^{-} = \sum_{m,n} n_{fi,m,n}^{-}, \tag{69}$$

$$g_i = \frac{\partial}{\partial \eta}(\ln n_{fi,m,n}^{+}) = -\frac{\partial}{\partial \eta}(\ln n_{fi,m,n}^{-}) \tag{70}$$

where the m and n indices denote the order of the transverse mode sustained (for each longitudinal mode – i) in the cavity under consideration.

Equations (68) and (70) should be solved together with the boundary condition (20) and with the relations between the incident and reflected light intensities on the cavity mirror surfaces, rewritten in the new forms:

$$a_{m,n} R^{+} n_{fi,m,n}^{+}(\xi, 1) = n_{fi,m,n}^{-}(\xi, 1), \tag{71}$$

$$a_{m,n} R^{-} n_{fi,m,n}^{-}(\xi, 0) = n_{fi,m,n}^{+}(\xi, 0). \tag{72}$$

The factors $a_{m,n}$ appearing in Eqs. (71) and (72) measure the individual (m,n) transverse mode diffractional losses. Based on the data gathered in [9] and [10] these factors can be defined by the relation

$$a_{m,n} = \exp[J_m(2\chi_{m,n})] \tag{73}$$

where

$$\chi_{m,n} = \frac{1}{2}\left[\left(\frac{\pi m}{M_x + i\gamma}\right)^2 + \left(\frac{\pi n}{M_z + i\gamma}\right)^2\right] \tag{74}$$

$M_x = (2kL_x^2/L_y)$ and $M_z = (2kL_z^2/L_y)$ in Eq. (74) are proportional to the square roots of the respective Fresnel numbers; γ is a complex number assumed (after [11]) as equal to $\gamma \simeq 0.824\ (1-i)$.

The formal procedure leading to the solution of Eqs. (68) and (71) remains identical as that used in the precedent sections of this paper. For any given transverse mode (m,n), and for any given i-th line, the equations describing the changes of the respective photon number densities $n^{+,-}_{fi,m,n}$ have the following forms:

$$\frac{\partial^2 \ln n^+_{fi,m,n}}{\partial\xi\partial\eta} = -\Pi_{ci}\left[g_i \sum_{m,n}(n^+_{fi,m,n} + n^-_{fi,m}) + \sum_{j\neq i} g_j \sum_{m,n}(n^+_{fi,m,n} + n^-_{fj,m,n})\right], \tag{75}$$

$$\frac{\partial^2 \ln n^-_{fi,m,n}}{\partial\xi\partial\eta} = -\Pi_{ci}\left[g_i \sum_{m,n}(n^-_{fi,m,n} + n^-_{fi,m,n}) + \sum_{j\neq i} g_j \sum_{m,n}(n^+_{fj,m,n} + n^-_{fj,m,n})\right]. \tag{76}$$

Employing Eqs. (70) the Eqs (75) and (76) can be rewritten in the forms:

$$\frac{\partial}{\partial\eta}\left\{\frac{1}{\Pi_{ci}}\frac{\partial \ln n^+_{fi,m,n}}{\partial\xi} - \sum_{m,n}\left[(n^+_{fi,m,n} - n^-_{fi,m,n}) + \sum_{j\neq i}(n^+_{fj,m,n} - n^-_{fj,m,n})\right]\right\} = 0, \tag{77}$$

$$\frac{\partial}{\partial\eta}\left\{-\frac{1}{\Pi_{ci}}\frac{\partial \ln n^-_{fi,m,n}}{\partial\xi} - \sum_{m,n}\left[(n^+_{fi,m,n} - n^-_{fi,m,n}) + \sum_{j\neq i}(n^+_{fj,m,n} - n^-_{fj,m,n})\right]\right\} = 0. \tag{78}$$

The ratio intensities of two arbitrary chosen lines i and j can be treated as given by Eqs. (34) and (35) for each pre-set transverse mode (m,n). By putting into approximative formulae (34) and (35) $\bar{g}_i = \bar{g}_j = 0$ and introducing them into Eqs. (77) and (78) we obtain

$$\frac{\partial}{\partial\eta}\left[\frac{1}{\Pi_{ci}}\frac{\partial \ln n^+_{fi,m,n}}{\partial\xi} - \sum_{m,n}\{n^+_{fi,m,n}[1 + \sum_{j\neq i} A^+_{fj,i}(\xi,\eta/\eta)] - n^-_{fi,m,n}[1 + \sum_{j\neq i} A^-_{fj,i}(\xi,\eta/\eta)]\}\right] = 0, \tag{79}$$

$$\frac{\partial}{\partial\eta}\left[\frac{1}{\Pi_{ci}}\frac{\partial \ln n^-_{fi,m,n}}{\partial\xi} - \sum_{m,n}\{n^-_{fi,m,n}[1 + \sum_{j\neq i} A^-_{fji}(\xi,\eta/\eta)] - n^+_{fi,m,n}[1 + \sum_{j\neq i} A^+_{fj,i}(\xi,\eta/\eta)]\}\right] = 0. \tag{80}$$

In what follows it is assumed that for each individual i-th line the ratio(s) of the radiation field intensities pertaining to (m,n) and (r,s) transverse modes remains constant and equal to

$$n^+_{fi,m,n}/n^+_{fi,r,s} = n^-_{fi,m,n}/n^-_{fi,r,s} = a^{m,n}_{r,s} = a_{m,n}/a_{r,s}. \tag{81}$$

Using Equation (81) one can transform Eqs. (79) and (80) into the final form of

equations describing the changes in photon-number density for each individual line and each arbitrary (m,n) transverse mode pertaining to the line in question we have:

$$\frac{\partial}{\partial\eta}\left\{\frac{1}{\Pi_{ci}}\frac{\partial \ln n^{+}_{fi,m,n}}{\partial\xi} - n^{+}_{fi,m,n}[(1+\sum_{r\neq m} a^{r,s}_{m,n}) + \sum_{j\neq i} A^{+}_{fj,i}(\xi,\eta/\eta)(1+\sum_{\substack{r\neq m\\ s\neq n}} a^{r,s}_{m,n})]\right.$$
$$\left. + n^{-}_{fi,m,n}[(1+\sum_{\substack{r\neq m\\ s\neq n}} a^{r,s}_{m,n}) + \sum_{j\neq i} A^{-}_{fj,i}(\xi,\eta/\eta)(1+\sum_{\substack{r\neq m\\ s\neq n}} a^{r,s}_{m,n})]\right\} = 0, \tag{82}$$

$$\frac{\partial}{\partial\eta}\left\{\frac{1}{\Pi_{ci}}\frac{\partial \ln n^{-}_{fi,m,n}}{\partial\xi} + n^{+}_{fi,m,n}[(1+\sum_{\substack{r\neq m\\ s\neq n}} a^{r,s}_{m,n}) + \sum_{j\neq i} A^{+}_{fj,i}(\xi,\eta/\eta)(1+\sum_{\substack{r\neq m\\ s\neq n}} a^{r,s}_{m,n})]\right.$$
$$\left. - n^{-}_{fi,m,n}[(1+\sum_{\substack{r\neq m\\ s\neq n}} a^{r,s}_{m,n}) + \sum_{j\neq i} A^{-}_{fj,i}(\xi,\eta/\eta)(1+\sum_{\substack{r\neq m\\ s\neq n}} a^{r,s}_{m,n})]\right\} = 0. \tag{83}$$

Employing boundary conditions (71) and (72) together with Eqs. (70), Eqs. (82) and (83) can be reduced to Bernoulli's equations:

$$\frac{dA^{+}_{fi,m,n}}{d\xi} = -n^{+}_{fi,m,n}(\xi,1)\,\Pi_{ci}(1+\sum_{\substack{r\neq m\\ s\neq n}} a^{r,s}_{m,n})\left[\left(A^{+}_{fi,m,n}\right)^2[1+\sum_{j\neq i} A^{+}_{fj,i}(\xi,\eta/\eta)]\right.$$
$$-\{[1+\sum_{j\neq i} A^{+}_{fj,i}(\xi,1/1)] + a_{m,n}R^{+}[1+\sum_{j\neq i} A^{-}_{fj,i}(\xi,1/1)]\}$$
$$\left.\times A^{+}_{fi,m,n} - a_{m,n}R^{+}[1+\sum_{j\neq i} A^{-}_{fj,i}(\xi,\eta/\eta)]\right] = 0, \tag{84}$$

$$\frac{dA^{-}_{fi,m,n}}{d\xi} = -n^{-}_{fi,m,n}(\xi,0)\,\Pi_{ci}(1+\sum_{\substack{r\neq m\\ s\neq n}} a^{r,s}_{m,n})\left[\left(A^{-}_{fi,m,n}\right)^2[1+\sum_{j\neq i} A^{-}_{fj,i}(\xi,\eta/\eta)]\right.$$
$$-\{[1+\sum_{j\neq i} A^{-}_{fj,i}(\xi,0/0)] + a_{m,n}R^{-}[1+\sum_{j\neq i} A^{+}_{fj,i}(\xi,0/0)]\}$$
$$\left.\times A^{-}_{fi,m,n} - a_{m,n}R^{-}[1+\sum_{j\neq i} A^{+}_{fj,i}(\xi,\eta/\eta)]\right] = 0. \tag{85}$$

Solving Equations (84) and (85) subject to boundary conditions (20), (71) and (72) one obtains that on the resonator mirror surface

$$n^{+}_{fi,m,n}(\xi,1) = \|n^{+}_{fi,m,n}(\xi,1)\|\,\delta_{\mathrm{D}}(\xi) \quad \text{and} \quad n^{-}_{fi,m,n}(\xi,0) = \|n^{-}_{fi,m,n}(\xi,0)\|\,\delta_{\mathrm{D}}(\xi).$$

The respective norms follow the relations

$$\|n^{+}_{fi,m,n}(\xi,1)\| = \frac{2}{\Pi_{ci}(1+\sum_{\substack{r\neq m\\ s\neq n}} a^{r,s}_{m,n})[1+\sum_{j\neq i}(\xi,0/0)]\,[x^{+}_{1i,m,n}(0) - x^{+}_{2i,m,n}(0)]}$$
$$\times \ln\left[\frac{\exp(-\Pi_{vi}) - x^{+}_{1i,m,n}(0)}{\exp(-\Pi_{vi}) - x^{+}_{2i,m,n}(0)}\,\frac{x^{+}_{2i,m,n}(0) - a_{m,n}\sqrt{R^{+}R^{-}}}{x^{+}_{1i,m,n}(0) - a_{m,n}\sqrt{R^{+}R^{-}}}\right], \tag{86}$$

$$\|n^-_{fi,m,n}(\xi,0)\| = \frac{2}{\Pi_{ci}(1+\sum_{\substack{r\neq m\\ s\neq n}} a^{r,s}_{m,n})[1+\sum_{j\neq i} A^-_{fj,i}(\xi,1/1)]\,[x^-_{1i,m,n}(1)-x^-_{2i,m,n}(1)]}$$

$$\times \ln\left[\frac{\exp(-\Pi_{vi})-x^-_{1i,m,n}(1)\,x^-_{2i,m,n}(1)-a_{m,n}\sqrt{R^+R^-}}{\exp(-\Pi_{vi})-x^-_{2i,m,n}(1)\,x^-_{1i,m,n}(1)-a_{m,n}\sqrt{R^+R^-}}\right]. \tag{87}$$

In Equations (86) and (87), $x_{1,2,i,m,n}(\eta)$ indicate the roots of two following algebraic equations:

$$x^2[1+\sum_{j\neq i} A^+_{fj,i}(\xi,\eta/\eta)]-x\{[1+\sum_{j\neq i} A^+_{fj,i}(\xi,1/1)]$$

$$+a_{m,n}R^+[1+\sum_{j\neq i} A^-_{fj,i}(\xi,1/1)]\}-a_{m,n}R^+[1+\sum_{j\neq i} A^-_{fj,i}(\xi,\eta/\eta)]=0,$$

$$x^2[1+\sum_{j\neq i} A^-_{fj,i}(\xi,\eta/\eta)]-x\{[1+\sum_{j\neq i} A^-_{fj,i}(\xi,0)]$$

$$+a_{m,n}R^-[1+\sum_{j\neq i} A^+_{fj,i}(\xi,0/0)]\}-a_{m,n}R^-[1+\sum_{j\neq i} A^+_{fj,i}(\xi,\eta/\eta)]=0.$$

Relations (86) and (87) being given the problem can be treated as formally closed as their knowledge permits us to calculate any desired output power characteristic of the multi-line, multi-transverse mode cw gasdynamic laser cavity.

4.2. Main power characteristics

The virtual radiation power brought to the cavity inlet cross-section ($\xi = 0$) remains defined by the previously given relation (52). The measure of the single-line, single-transverse mode output power, defined under assumption that light intensity deflected due to diffraction should be considered as lost, follows the formula

$$\overline{p_{fi,m,n}(\mathbf{G})} = \frac{1}{2}\frac{v_i}{\langle v_i\rangle}[(1-R^+)\|n^+_{fi,m,n}(\xi,1)+(1-R^-)\|n^-_{fi,m,n}(\xi,0)\|].$$

Using the solutions (86) and (87) the last relation can be rewritten in the following form:

$$\overline{p_{fi,m,n}(\mathbf{G})} = \left[\frac{\exp(-\Pi_{vi})-x^+_{1i,m,n}(0)\,x^+_{2i,m,n}(0)-a_{mn}\sqrt{R^+R^-}}{\exp(-\Pi_{vi})-x^+_{2i,m,n}(0)\,x^+_{1i,m,n}(0)-a_{mn}\sqrt{R^+R^-}}\right]^{\alpha}$$

$$\times\left[\frac{\exp(-\Pi_{vi})-x^-_{1i,m,n}(1)\,x^-_{2i,m,n}(1)-a_{m,n}\sqrt{R^+R^-}}{\exp(-\Pi_{vi})-x^-_{2i,m,n}(1)\,x^-_{1i,m,n}(1)-a_{m,n}\sqrt{R^+R^-}}\right]^{\beta} \tag{88}$$

where

$$\alpha = \frac{\nu_i}{\langle \nu_i \rangle} \frac{1}{\Pi_{ci}} \frac{1 - R^+}{(1 + \sum_{\substack{r \neq m \\ s \neq n}} a^{r,s}_{m,n})[1 + \sum_{j \neq i} A^+_{fj,i}(\xi, 0/0)][x^+_{1i,m,n}(0) - x^+_{2i,m,n}(0)]}. \tag{89}$$

$$\beta = \frac{\nu_i}{\langle \nu_i \rangle} \frac{1}{\Pi_{ci}} \frac{1 - R^-}{(1 + \sum_{\substack{r \neq m \\ s \neq n}} a^{r,s}_{m,n})[1 + \sum_{j \neq i} A^+_{fj,i}(\xi, 1/1)][x^-_{1i,m,n}(1) - x^-_{2i,m,n}(1)]}. \tag{90}$$

In Equations (88)–(90):

$$x^+_{1i,m,n}(0) = x^-_{2i,m,n}(1) = \frac{1 + \sum_{j \neq i} \frac{f_m(T_0, J_j)\, \mathscr{L}(\nu, \nu_i)}{f_m(T_0, J_i)\, \mathscr{L}(\nu, \nu_j)}}{1 + \sum_{j \neq i} \frac{f_m(T_0, J_j)\, \mathscr{L}(\nu, \nu_i)}{f_m(T_0, J_i)\, \mathscr{L}(\nu, \nu_j)} \exp[-(\Pi_{vj} - \Pi_{vi})]}, \tag{91}$$

$$x^+_{2i,m,n}(0) = -a_{m,n} R^+, \quad x^-_{2i,m,n}(1) = -a_{m,n} R^-. \tag{92}$$

The single-line (i), single-transverse mode (m, n) load coefficient $\mathfrak{k}_{fi,m,n}(\mathbf{G})$ can be thus expressed by the relation

$$\mathfrak{k}_{fi,m,n}(\mathbf{G}) = \Pi_{ii} \frac{\Pi_{ci}}{\Pi_{vi}} \ln \overline{p_{fi,m,n}(\mathbf{G})}. \tag{93}$$

Similarly, the single-line efficiency and the overall efficiency of the cavity are given by the respective formulae:

$$\mathfrak{k}_{fi}(\mathbf{G}) = \sum_{m,n} \mathfrak{k}_{fi,m,n}(\mathbf{G}) = \ln \prod_{m,n} [\overline{p_{fi,m,n}(\mathbf{G})}]^{\Pi_{ii}\Pi_{ci}/\Pi_{vi}}, \tag{94}$$

$$\eta_f(\mathbf{G}) = \sum_i \mathfrak{k}_{fi}(\mathbf{G}) = \ln \prod_{i,m,n} [\overline{p_{fi,m,n}(\mathbf{G})}]^{\Pi_{ii}\Pi_{ci}/\Pi_{vi}}. \tag{95}$$

In relations (94) and (95) the summation and multiplication are extended over the values of indexes i, m, n for which the $\mathfrak{k}_{fi,m,n}(\mathbf{G})$ remains higher than zero. In view of (88) and (93) this occurs when

$$\exp(-\Pi_{vi}) < \sqrt{x^+_{2i,m,n}(0)\, x_{2i,m,n}(1)} < x^+_{1i,m,n}(0) = x^-_{1i,m,n}(1). \tag{96}$$

By comparing the last formula with an analogous one given in [1] for a single-transverse mode multiline cavity, it can be noticed that for each (m, n) mode the i-th line can be sustained within the narrower range of the cavity losses. The i-th line appears if $\ln(\sqrt{R^+ R^-})^{-1}$ becomes lower than $\Pi_{vi} - J_m(2\chi_{m,n})$ and is switched-off (due to the process of maxwellization of the rotational energy distribution function [1]) if $\ln(\sqrt{R^+ R^-})^{-1}$ becomes equal to $x^+_{1i,m,n}(0) - J_m(2\chi_{m,n}) = x^-_{1i,m,n}(1) - J_m(2\chi_{m,n})$. For typical cavities of CW-GDL this narrowing of the admissible range of $\sqrt{R^+ R^-}$ values is almost negligible as the values of M_x and/or M_z numbers are

generally very high. In this case $J_m(2\chi_{m,n}) = 0(2\pi^2 q^2 \mathrm{Re}\gamma/M^3)$ ($q = m$ or n) and $M = M_x$ or M_z, respectively, and for very large number of transverse modes the coefficient $a_{m,n}$ remains close to one. The relation (96) permits us to identify the number of transverse modes into which each individual line intensity is split; with that number being known the output beam energy distribution over the single-line, single-transverse mode composite fractions can be calculated from the relation (93). It may be suggested that the rate equation approach to this problem can be useful in establishing an initial form of the field distribution over the cavity mirror, thus reducing the number of numerical steps needed in lengthy iterative methods leading to the solution of the same problem on the basis of Maxwell equations [10], [12].

4.3. Numerical example

The numerical example concerns the same CW-GDL which was discussed in Section 3.5 of this paper. The values of characteristic parameters Π_{vi}, Π_{ci}, Π_{ii}, $v_i/\langle v_i \rangle$ are listed in Tables 1 and 2. The limited number of values of the transverse mode diffractional losses measure $a_{m,n}$ are gathered in Tab. 3. In calculations concerning the cavity efficiencies, 60 P-branch and R-branch lines and $m,n = 1,2,\ldots,30$ different transverse modes were considered. From Tab. 3 it is evident that the $a_{m,n}$ values remain (as expected) close to one for very high number of transverse modes. The behaviour of transverse mode load coefficient $\mathfrak{k}_{fi,m,n}(\mathbf{G})$ is (for few

Table 3. Transverse mode diffractional losses measure $a_{m,n}$

n \ m	1	2	3	4	5	6	7	8	9
1	.999	.998	.997	.994	.992	.988	.984	.979	.974
2	.999	.998	.997	.994	.992	.988	.984	.979	.974
3	.999	.998	.997	.994	.992	.988	.984	.979	.974
4	.999	.998	.997	.994	.992	.988	.984	.979	.974
5	.999	.998	.997	.994	.992	.988	.984	.979	.974
6	.999	.998	.997	.994	.992	.988	.984	.979	.974
7	.999	.998	.997	.994	.992	.988	.984	.979	.974
8	.999	.998	.997	.994	.992	.988	.984	.979	.974
9	.999	.998	.997	.994	.992	.988	.984	.979	.974
10	.999	.998	.997	.994	.992	.988	.984	.979	.974

longitudinal modes) shown in Fig. 5 (for the case of lack of pumping and relaxation processes), and in Fig. 6 (for the case of ideal pumping and relaxation). The overall efficiency $\eta_f(\mathbf{G})$ (see Eq. (95)) of the multi-line, multi-transverse mode cavity was reported in [5], where it has been shown that the influence of the transverse mode diffractional losses onto the CW-GDL overall net output is for high Fresnel number almost negligible.

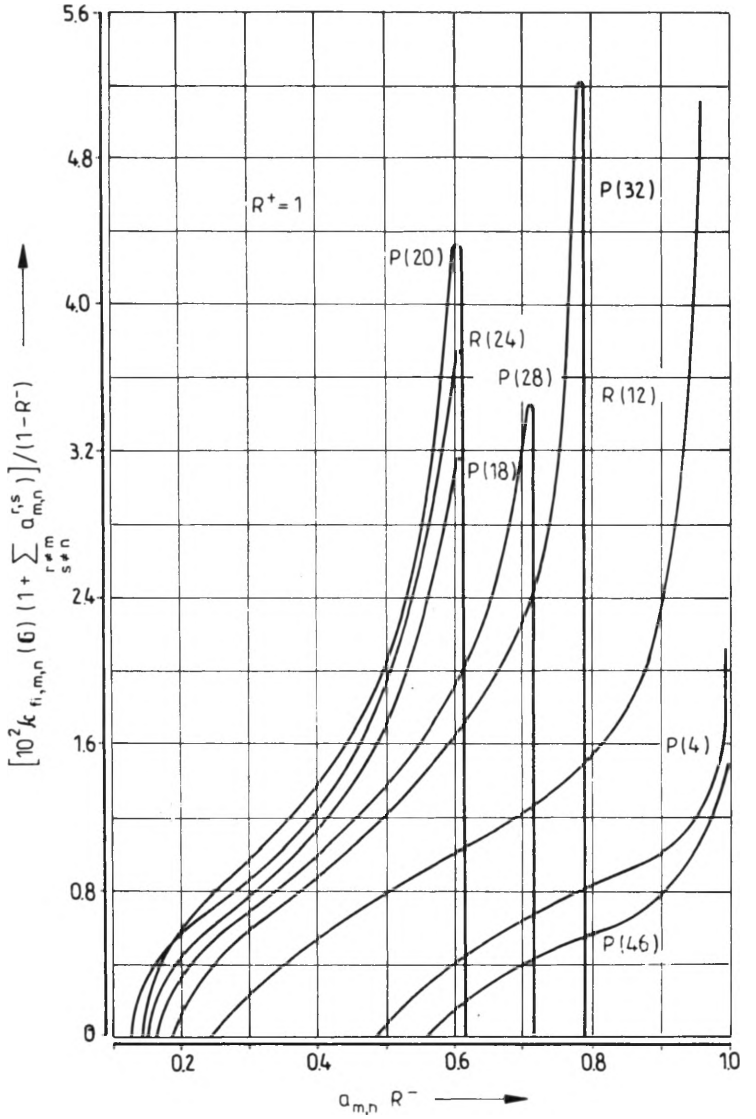

Fig. 5. Single tansverse mode load coefficient (efficiency) $\mathfrak{k}_{fi,m,n}(\mathbf{G})$ for the case of negligible pumping and relaxation

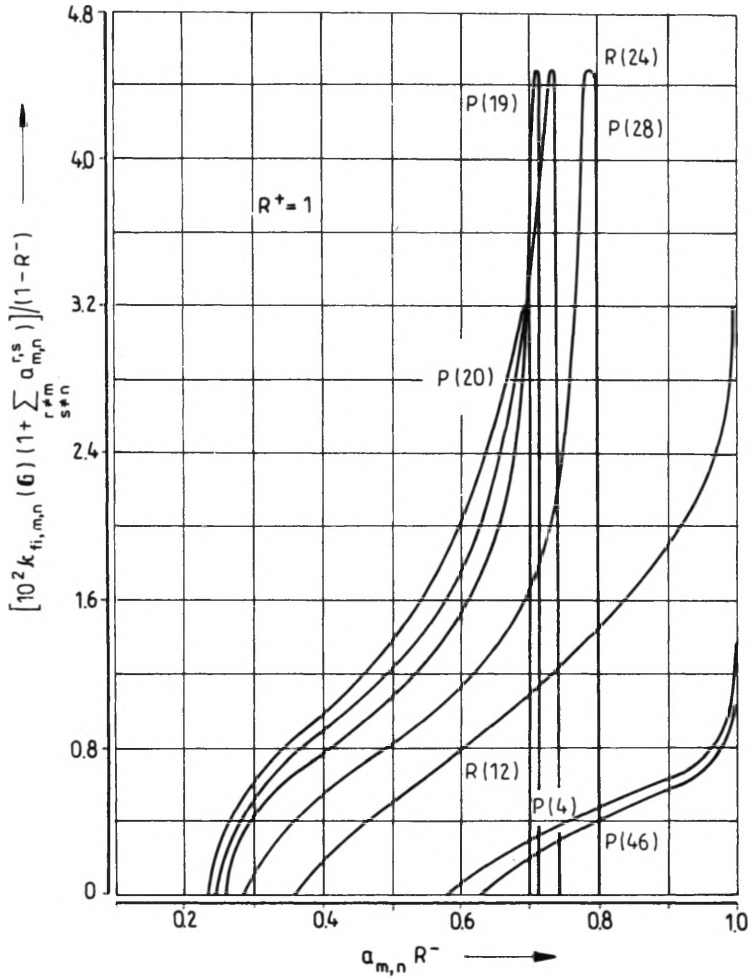

Fig. 6. Single transverse mode load coefficient (efficiency) $\mathring{t}_{fi,m,n}(G)$ for the case of ideal pumping and relaxation

5. Closing remarks

The principal aim of this paper consisted in giving a set of simplified analytical formulae for multiline cw gasdynamic laser averaged power characteristics as related to the effects of line self- and cross-saturation and to the multi-transverse mode diffractional losses. It is believed that these formulae can be useful in selecting the cavity for CW-GDL and in estimating its expected net output power. It is further expected that the formulae discussed in this paper can offer a rough insight into some basic physical processes pertinent to the CW-GDL operation. It is finally suggested that the presented analytical results can be meaningful for CW-GDL cavities working in special conditions enforcing their single longitudinal and/or transverse

mode operation. The results reported previously in [5] show that the overall laser efficiency $\eta_f(\mathbf{G})$ is but slightly affected by line saturation and multi-transverse mode operation of its cavity. The problems of the line saturation and multi-transverse mode coexistence within the cavity under consideration were treated disjointly. By examining the structures of starting Eqs. (38), (39) and (84), (85) it can be noticed that the solutions describing the CW-GDL cavity working in multi-transverse mode regime in the case when the line saturation effects cannot be neglected, can be obtained directly from Eqs. (50), (51) by:

i) Multiplying each R^+ and R^- by $a_{m,n}$ (with exception of mirror reflectivities entering the formula (53)).

ii) Multiplying Π_{ci} by a factor $(1+\sum_{\substack{r\neq m\\ s\neq n}} a_{m,n}^{r,s})$.

Thus modified expressions will define the sought for value of the load coefficient(s) $\mathfrak{k}^{fi,m,n}(\mathbf{G})$.

The procedure of calculating laser output power characteristics remain identical with that described in Section 3.4. It ought to be remembered that equation used to determine the photon number density distribution over the mirrors surface have the form of pseudo-functions. The same remark applies to the gain spatial distribution. Therefore, they have only a heuristic meaning and attain the physical one after being averaged over the cavity region. According to test calculations [10], [12], thus obtained laser averaged characteristics bear an error equal to about 5–10% giving always underestimated values of laser efficiency and output power.

Acknowledgements – The author wishes to express his gratefulness to dr A. Zieliński from the Institute of Oceanology of the Polish Academy of Sciences in Sopot for his valuable help in preparing the numerical programs used in a part of this paper.

References

[1] BRUNNÉ M., MILEWSKI J., STAŃCO J., ZIELIŃSKI A., J. Appl. Phys. **47** (1976), 1385.
[2] RIGORD W. W., Appl. Phys. **39** (1965), 2487.
[3] ANDERSON J. D., Jr., *Gasdynamic Lasers: An Introduction*, Academic Press, New York 1976.
[4] MURRAY S., III, SCULLY M. D., LAM W. E., *Laser Physics*, Addison–Wesley Publ. Co., London 1974.
[5] BRUNNÉ M., ZIELIŃSKI A., [In] *Proc. Int. Conf. Laser '79*, G 9.
[6] HARRACH R. J., EINWOHNER T. M., Lawrance Livenore Laboratory Report No. UCRL–51399, 1973 (unpublished).
[7] BRUNNÉ M., MILEWSKI J., STAŃCO J., ZIELIŃSKI A., Bull. Acad. Pol. Sci. Techn. **20** (1972), 143.
[8] LEE G., Phys. Fluids **17** (1974).
[9] VAINSTEIN L. A., *Open Resonators and Wave-Guides*, Moscow 1966 (in Russian).
[10] RABCZUK G., IFFM Report No. 165/680, 1976 (unpublished).
[11] BRUNNÉ M., MILEWSKI J., STAŃCO J., ZIELIŃSKI A., AIAA Jour. **14** (1976), 352.
[12] RABCZUK G., MILEWSKI J., [In] *Proc. Int. Conf. Laser '79*, Orlando (Florida) 1979, T 12.

Received April 5, 1988
in revised form July 13, 1988

Влияние самонасыщения и сквозного насыщения линии, а также многомодной работы на энергетические характеристики активного резонатора газодинамического лазера постоянного действия

На базе системы макроскопических кинетических уравнений рассмотрена работа активного объемного резонатора CW-GDL в условиях сосуществования в нем многих продольных модов (линий) и поперечных. Целью разработки является приведение простых аналитических соотношений, связывающих выходную мощность и коэффициент полезного действия генерации CW-GDL с состоянием оптического возбуждения рабочей смеси при учете эффектов, связанных с само- и сквозным насыщениями линий и дифракционных потерь, сосуществующих в резонаторе многих поперечных модов. Полученные общие соотношения проиллюстрированы расчетным примером, выполненным для конвенционального CW-GDL, работающего на продуктах сгорания бензола в компрессорном воздухе.